Self-formed $In_xGa_{1-x}As$ Quantum Dot-like Laser Grown by Metal Organic Chemical Vapor Deposition on Si Substrate

3.1 Introduction

In laser diode fabrication, growth of island structures in the active region was demonstrated as an alternative approach to derive the reduced threshold current density and stability over temperature[1,2]. Among the 4 different type of island growth methods, the droplet epitaxy proved the difficulty in the optimization of uniform, size distributed islands with the adequate island density[1,2]. Apart from the droplet epitaxy Stransky-Krastanov (S-K) mode[3] seems another promising way to grow quantum dot (QD) or island in a lattice mismatch system. In this method, growth starts with an initial two dimensional layer and when the critical layer thickness is achieved, the surface transforms into three-dimensional islands due to the presence of high level strain in the interface between lattice mismatched systems. The transformed 3D islands continue to grow as dot structures coherently on the surface and the densely distributed coherent islands are achieved. This method is advantageous to grow islands with unique properties without the necessity of any micro-machining techniques like nanolithography or etching or implantation.

In the lattice-matched system, the mechanism for the self-ordering phenomena is faceting[4,5], where a planar crystal surface rearranges to a periodic hill-and-valley structure in order to decrease the surface energy[6]. Another class of effect is related to the formation of periodically ordered structures of surface domains, e.g., ordered arrays of monolayer-height islands in heterophase systems[7-9], or flat multilayer islands[10]. This ordering effect is realized by S-K growth mode in a lattice-mismatch system, caused by elastic relaxation due to the

discontinuity of the intrinsic surface stress tensor at facet edges and by strain-induced renormalization of the surface energy facet[11,12].

Due to the discrete energy levels in zero dimensional systems lower threshold current densities, higher characteristic temperatures and increased gain and differential gain in comparison with quantum well lasers are theoretically predicted[13,14]. Growth and study of self-formed quantum dot (QD) as well as fabrication of QD laser diodes are also in rapid progress in recent years[15-18]. Oshinowo et al. reported the growth of QD on GaAs with the density of ~10^9 - $10^{11}/cm^2$ by MOCVD[16]. InGaAs QD laser on GaAs substrate by MBE with low threshold current density is reported by Park et al[19]. But, there is few report[20] on the growth of QD as well as fabrication of QD laser on Si using S-K growth mode. Linder et al. reported the fabrication of self-organized $In_{0.4}Ga_{0.6}As$ QD lasers on Si substrate using S-K growth mode, which is able to lase only in the pulsed mode of operation[20]. The operation of QD laser diodes on Silicon substrate in the continuous wave (CW) operation is yet to realize.

In this chapter, the optimization of MOCVD growth parameters for growing QD structure using S-K growth mode is revealed in detail. The optimized growth condition was further used to fabricate QD-like laser diode on Si. The characteristics of the laser diodes were analyzed.

3.2 Experimental

3.2.1 Growth of quantum dot

The basic growth procedure except the growth of active regions of the laser diodes were carried out in the same manner as discussed in chapter 2, section 2.2.1. After loading the Si substrate in MOCVD reactor chamber, the substrates were heated in H_2 atmosphere at 1000°C for 10 minutes in order to remove the native oxide from the substrate surface. Then, a 2 μm thick GaAs buffer layer was

grown at 650°C. The growth of dots were carried out on the GaAs buffer layer by considering different parameters, such as total H_2 flow rate, growth temperature, AsH_3 flow rate, V/III ratio, growth time and In-compositions.

3.2.2 Fabrication of $In_{0.2}Ga_{0.8}As$ QD-like laser on Si

The QD like laser diode structure was fabricated by simply replacing the active region by the optimized QD like islands in the laser diode structure discussed in chapter 2, section 2.2.1 (Fig. 3.1). The QD like active region optimized for different In content (In=0.1, 0.2, 0.3, 0.4) were used to realize laser diodes.

3.2.3 Characterization Studies

Atomic force microscope (AFM) was used to check the surface morphology of the InGaAs epilayers on GaAs/Si. Injected current vs. output current (*I-L*) characteristics and emission spectrum analysis were carried out to observe the lasing property of the laser diode. Automatic power controlled (APC) lifetime measurement and electroluminescence (EL) topography has been performed in order to know the details on the degradation mechanism of laser diodes.

3.3 Results and Discussion

3.3.1 Characterization of $In_xGa_{1-x}As$ dots

The formation of $In_xGa_{1-x}As$ islands/dots on GaAs/Si depend on the growth conditions. Figure 3.2 shows the logarithmic plot of dot density as a function of growth temperature at fixed V/III ratio, In-content and growth time. It is observed that the dependence is not linear over the entire temperature range,

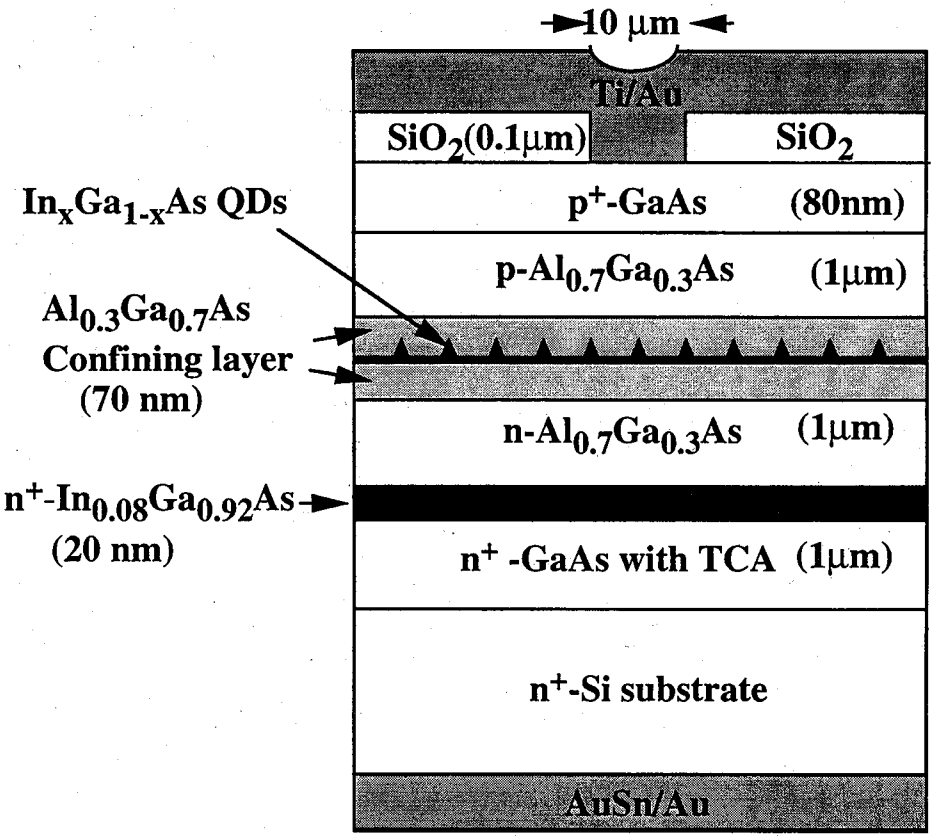

Figure 3.1 : Schematic structure of the $In_xGa_{1-x}As$ quantum dot-like laser on a Si substrate.

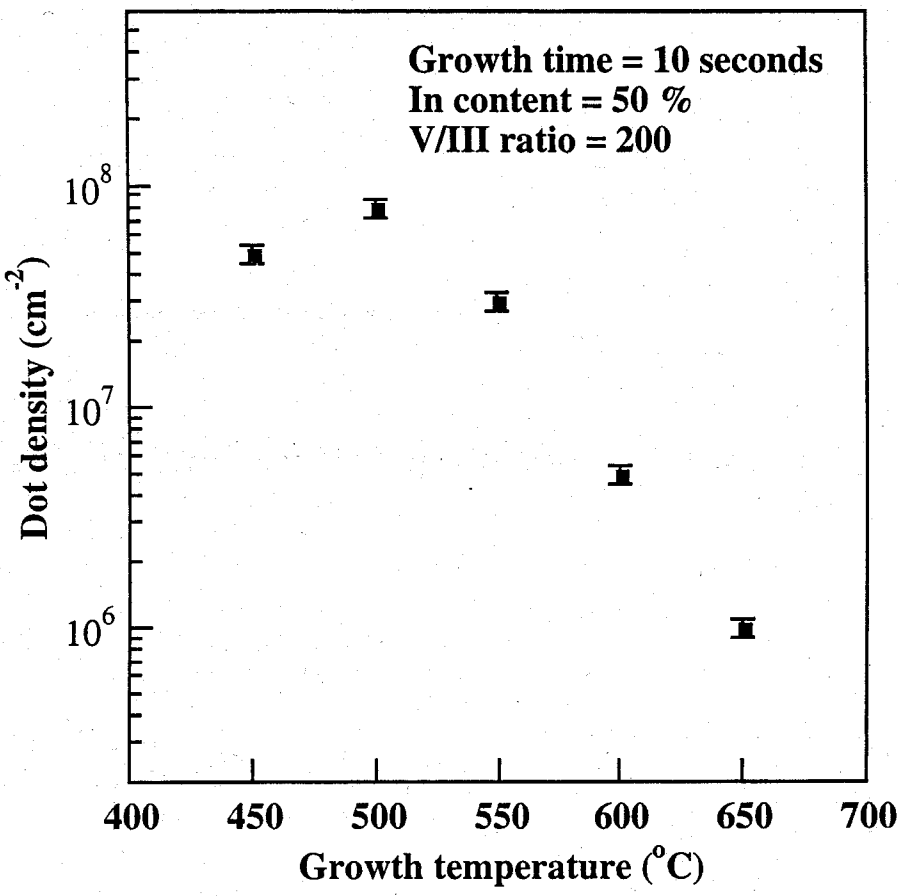

Figure 3.2 : Variation of dot density of InGaAs on Si substrate with respect to the growth temperatur e.

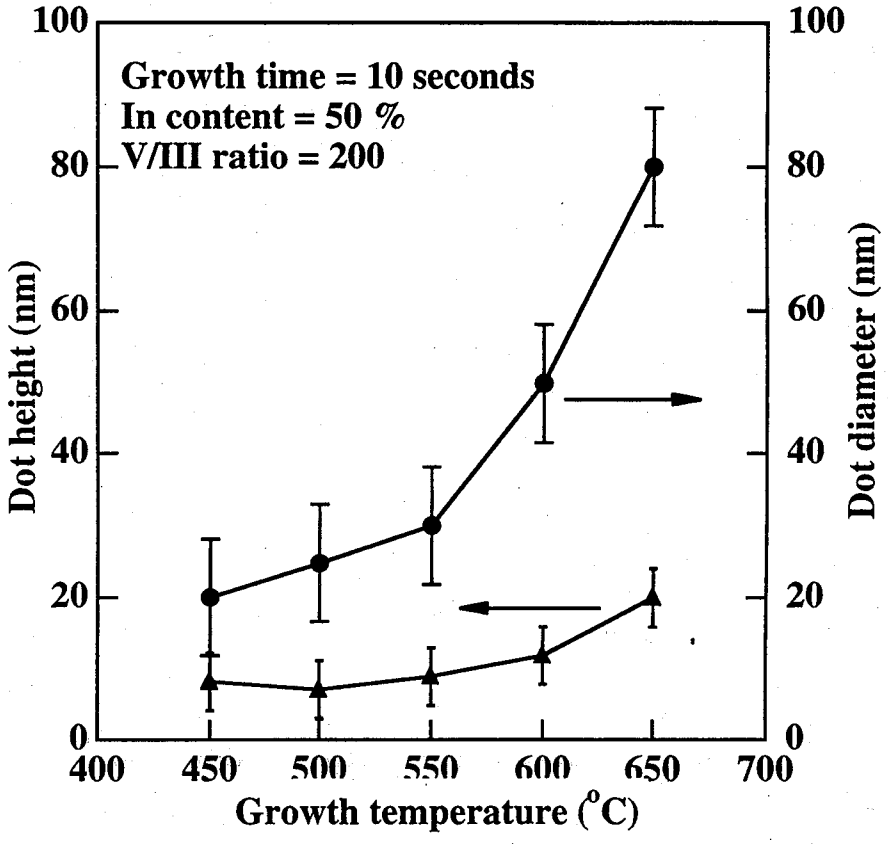

Figure 3.3 : Variation of dot diameter and height of InGaAs on Si substrate with respect to the growth temperature.

though a decrease in dot density with increasing temperature is revealed. This indicates that more than one kinetic process is competing to control the island formation of $In_xGa_{1-x}As$ on GaAs/Si. For instance, the arsenic incorporation behavior with Ga or In atom is different at the different growth temperatures above and below 500°C. Further, at the higher temperatures dots for at the defect sites, while, at the lower temperature dots are form due to the strain effect. The decrease in island density with increasing substrate temperature may be qualitatively reconciled as being a consequence of the thermally enhanced surface migration of In. The dependence of the dot heights and diameters as a function of growth temperature at fixed V/III ratio, In-content and growth time is shown in Fig. 3.3.

The dependence of dot density with respect to the variation of In-content at fixed growth temperature, time and V/III ratio is shown in Fig. 3.4 and the dependence of dot heights and diameters with respect to the variation of In-content at fixed growth temperature, time and V/III ratio is shown in Fig. 3.5. The figures reveal that there is an increase in dot density with the increase in In-content, but the size non-uniformity is severe in the case of higher percentage of In. In principle, In-content has an important role in the formation of islands since the formation of islands/dots by S-K growth mode is a strain-induced effect in a lattice-mismatch system. The bulk lattice mismatch of InAs and GaAs is ~7% and also there is a 4% lattice-mismatch in between GaAs and Si. As a result the strain distribution in the system of $In_xGa_{1-x}As$/GaAs/Si is more or less complicated. The AFM studies reveal that there are 2 types of growth mode operative depending upon the In content : 1) layer by layer growth mode below $x = 0.2$ and 2) 3D island growth mode above $x = 0.3$.

Further, the lower content of In results in discrete dots with an average inter dot distance of 2 μm in $In_{0.2}Ga_{0.8}As$ system (Fig. 3.6a). While for InAs (Fig. 3.6b) dots appear locally connected in agglomerations. The above such observation

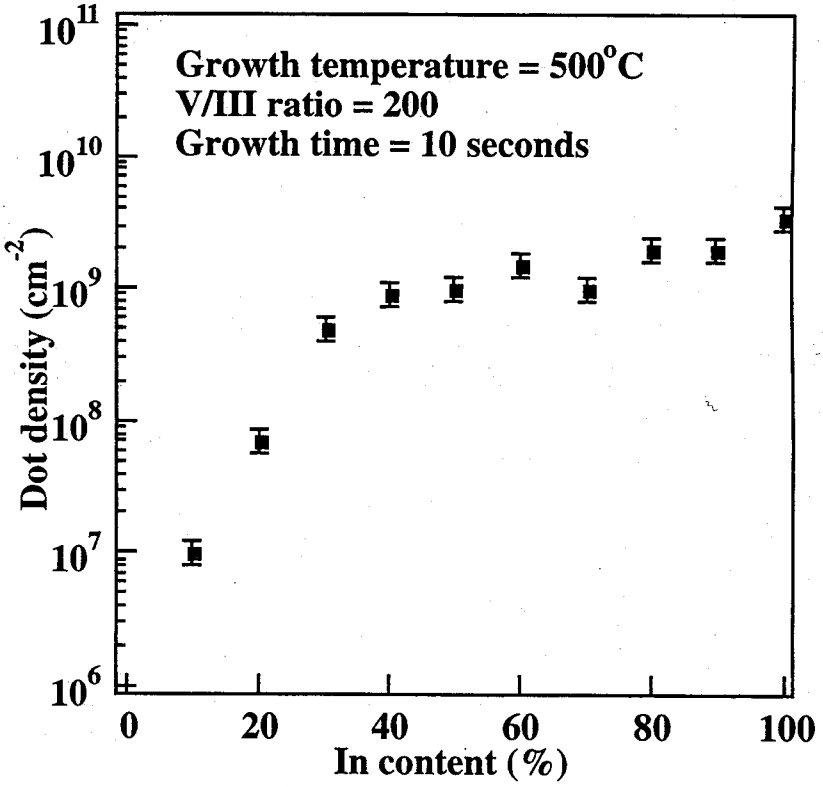

Figure 3.4 : Variation of dot density of InGaAs on Si substrate with respect to In content.

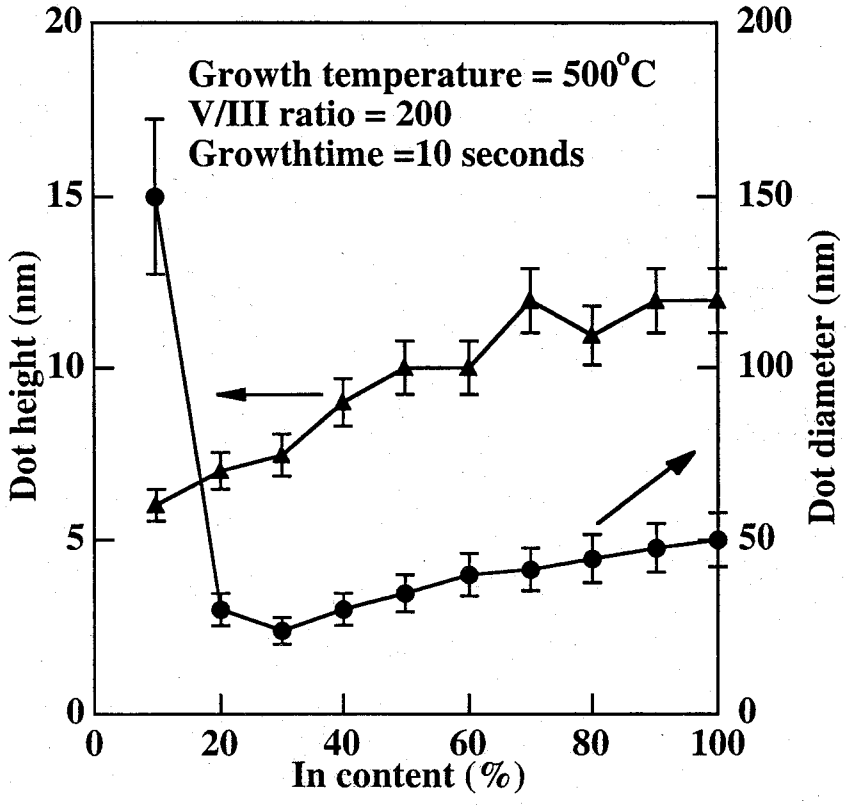

Figure 3.5 : Variation of dot height and diameter of InGaAs on Si substrate with respect to In content.

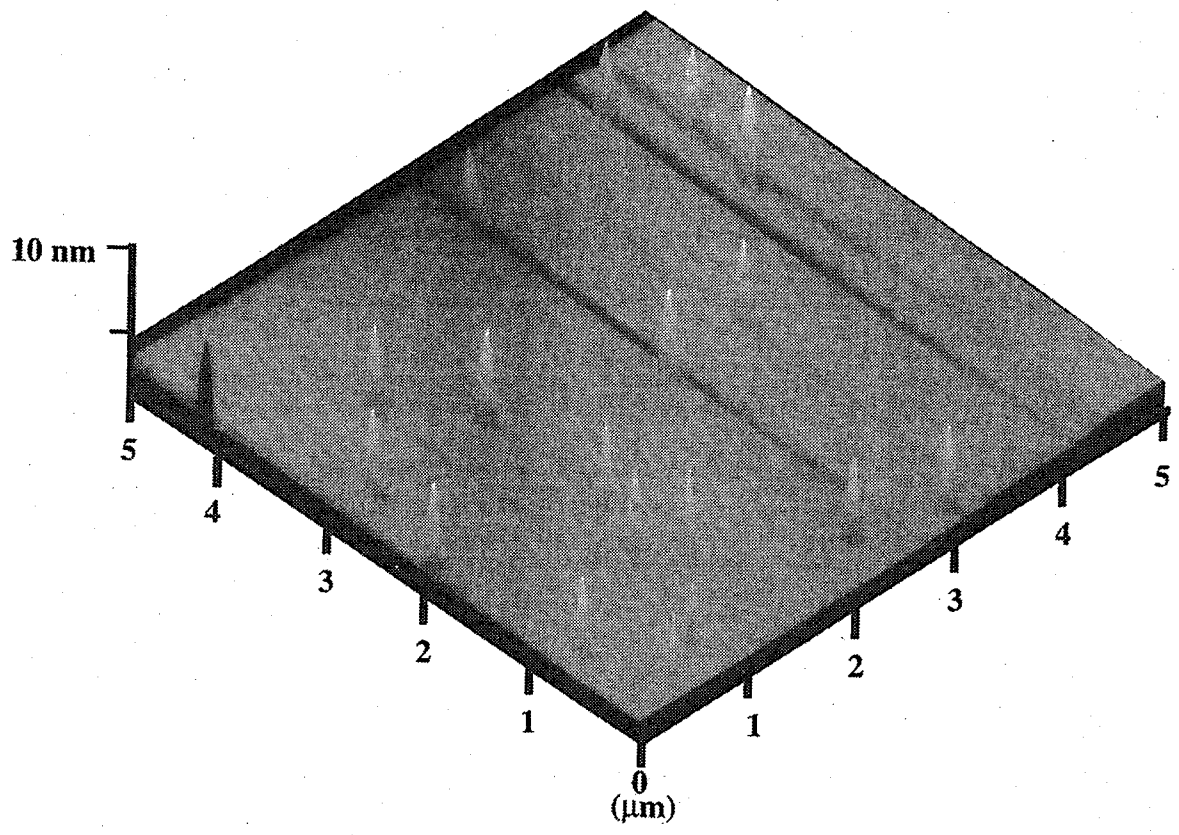

(a)

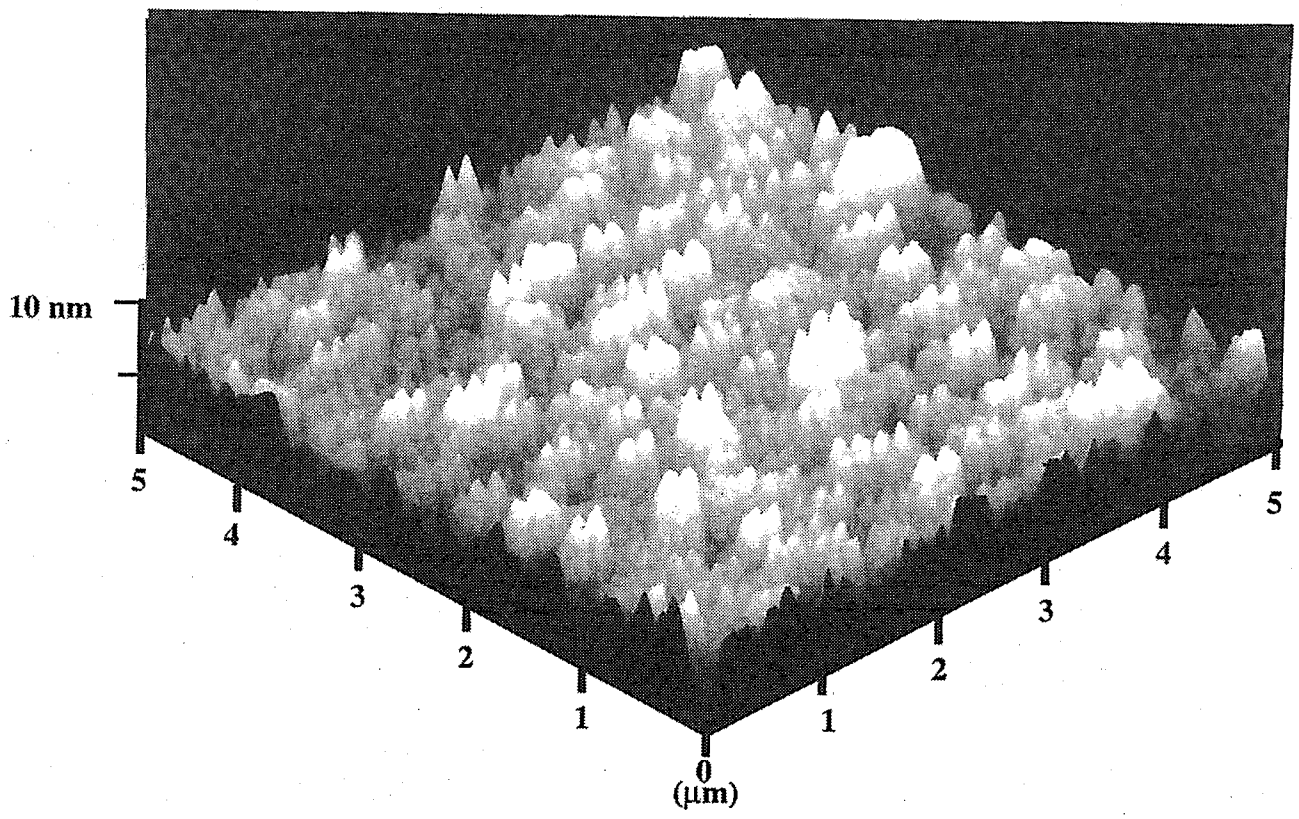

(b)

Figure 3.6 : AFM images of typical InGaAs dot on Si with In content (a) 20 %, (b) 100 %.

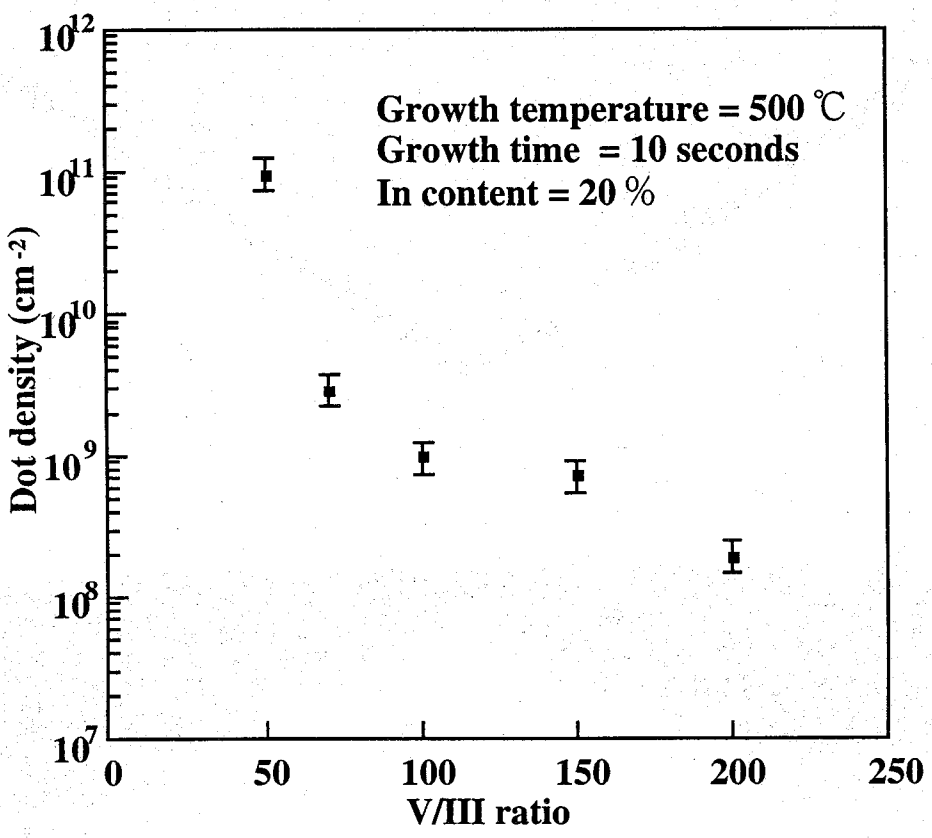

Figure 3.7 : Variation of dot density of InGaAs on Si with respect to group V/III ratio.

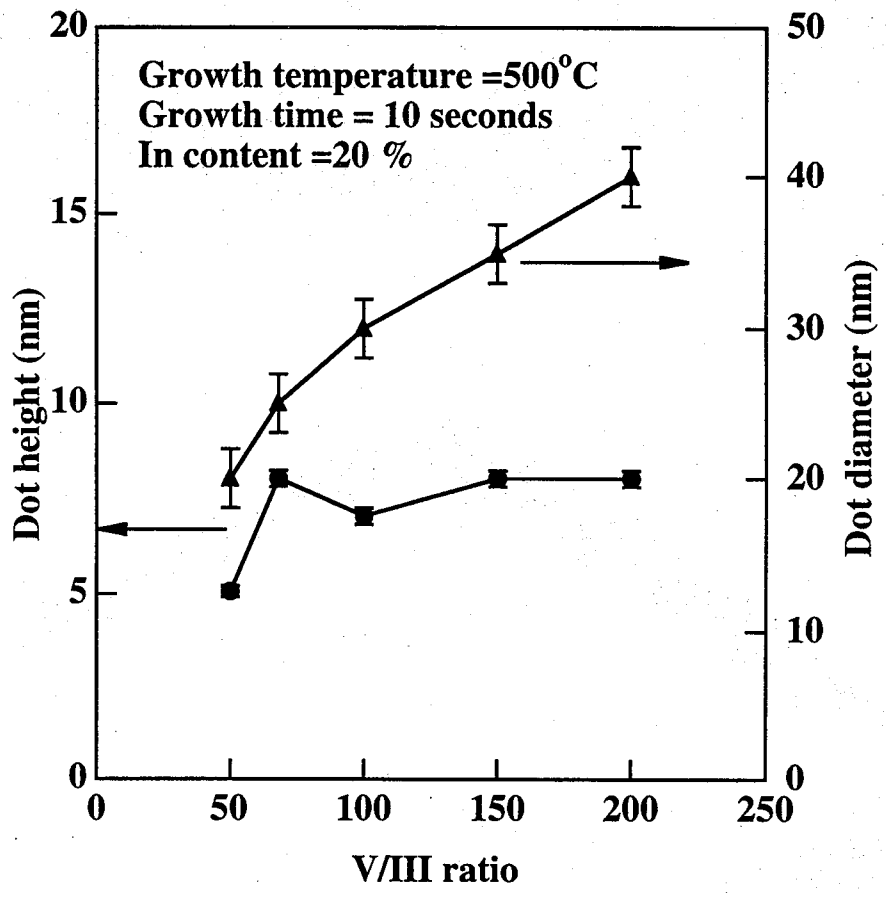

Figure 3.8 : Variation of dot diameter and height of InGaAs on Si substrate with respect to V/III ratio.

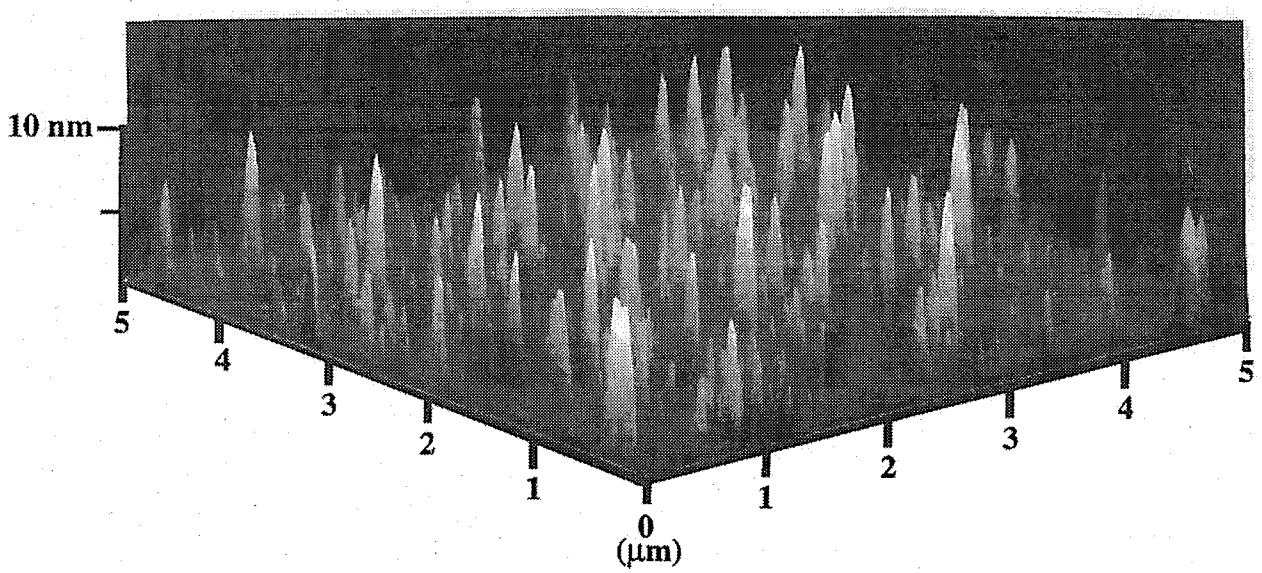

(a)

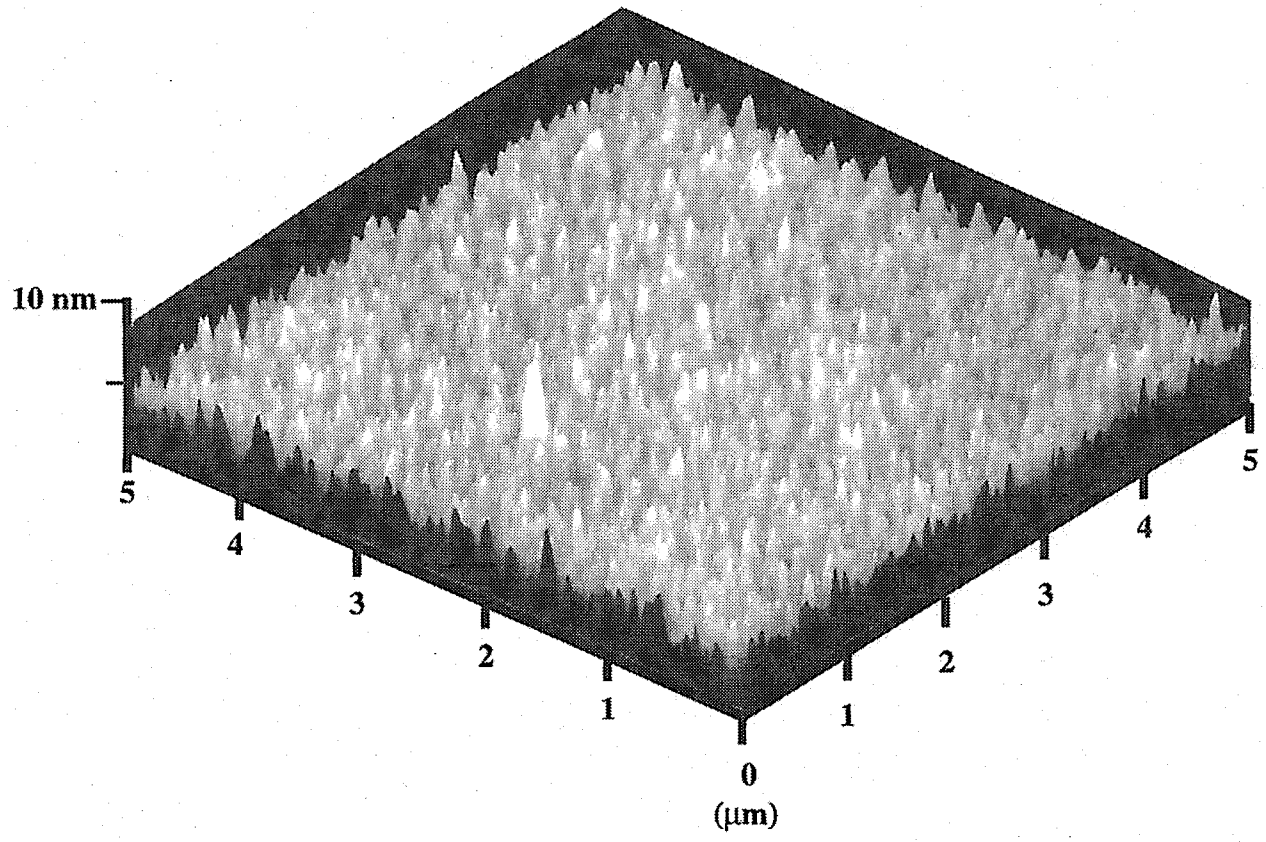

(b)

Figure 3.9 : AFM images of typical $In_{0.2}GaAs$ dot on Si with V/III ratio (a) 68, (b) 50 %.

once again implies that the onset of dot formation is governed by strain energy[11,12].

The growth of islands is also depend upon the V/III ratio, which controls the availability of the constituents for the growth. The As, Ga and In reaches the growing islands via intraplanar surface migration. Even for sufficient intraplanar migration of Ga and In , the ability of the both is an important parameter to be considered. Figure 3.7 shows the variation of dot density of InGaAs on Si with respect to group V/III ratio. It is found that as the V/III ratio decreases, the dot density increases. But, too much reduction in the V/III ratio results in overlapping of the dots. The size variations of the dots for the different V/III ratio is shown in Fig. 3.8. Figure 3.9 shows the AFM images of InGaAs QD on Si for two different V/III ratios (a. 68 and b. 50). In case of Fig. 3.9a (68 of V/III ratio) the dots are discrete with a dot density of ~ $10^9/cm^2$ and an inter-dot mean distance is 400 nm, where as in Fig.3.9b (50 of V/III ratio),the dots are interlinked and in some places overlapped with a density of ~10^{11} /cm^2. Even though the dot density is higher in the second case, the dots are shapeless to consider as quantum dots. From the crystal growth point of view, the growth rate is controlled by the group-III flux whose incorporation is unity and the growth kinetics is controlled by the adsorption rate of group-V elements. In case of higher V/III ratio, the As incorporation rate become slow, since group-III migration inhibits the subsequent arrival of additional group-III atoms due to the allotment of the sites for As incorporation and which results in discrete QD growth. On the other hand, in case of extremely lower V/III ratio, the unavailability of As leads to the formation of Ga or In rich droplets and the extension of its size makes them to joint together due to the higher wetting capability. So, the droplets are not discrete in nature and it is believed that they are not useful for the further application of QD device fabrication. The observation of very high dot density may not be also real due to the inter-linked nature of the dots.

3.3 .2 Characterization of $In_xGa_{1-x}As$ QD-like laser on Si

Lasing characteristics were carried out for the lasers with QD-like active region containing InGaAs (In = 10, 20, 30, 40%). It is notable the formation of dot was not realized with the In content 10%. Figure 3.10 shows the typical Injection current versus light output (*I-L*) characteristics of $In_{0.1}Ga_{0.9}As$ laser measured at RT under CW condition. The emission spectrum is also shown in the inset of Fig. 3.10. This laser shows a threshold current density of 2.15 kA/cm^2 with an external differential quantum efficiency of 11%. Ground state emission at 855 nm.

I-L characteristics of the laser with $In_{0.2}Ga_{0.8}As$ QD-like active region measured at RT, under CW condition is shown in Fig. 3.11. The measurement reveals that the threshold current density is 1.32 kA/cm^2 with an external differential quantum efficiency of 32%. This threshold current density is comparatively lower than the GaAs-based quantum well laser on Si[21]. An ideally low dimensional QD as the gain medium is expected to results in an ultra-low threshold current by modifying the density of states function and differential gain. But, in practice, the size fluctuation of the dots gives severe effect on the threshold current density. Further, the dots are accompanied by a two dimensional layer called a wetting layer, which is acting as a relaxing medium for the diffusively injected carriers through the barrier layer. Some carriers recombine radiatively or non-radiatively both outside (wetting layer) and inside the dots. The injected carriers in to the ground state emit photons to the lasing mode primarily due to the stimulated emission process. Whereas the carrier injection in to the higher energy levels have a higher probability of non-radiative recombination due to an increased number of recombination path. The properly sized QDs results in lower defect density and enhances the carrier injection from the ground state. If the presence of non-radiative recombination centers are eliminated from the dots the threshold current density is substantially reduced. The observation of reduced threshold current density for the QD-like laser diode is in good agreement with

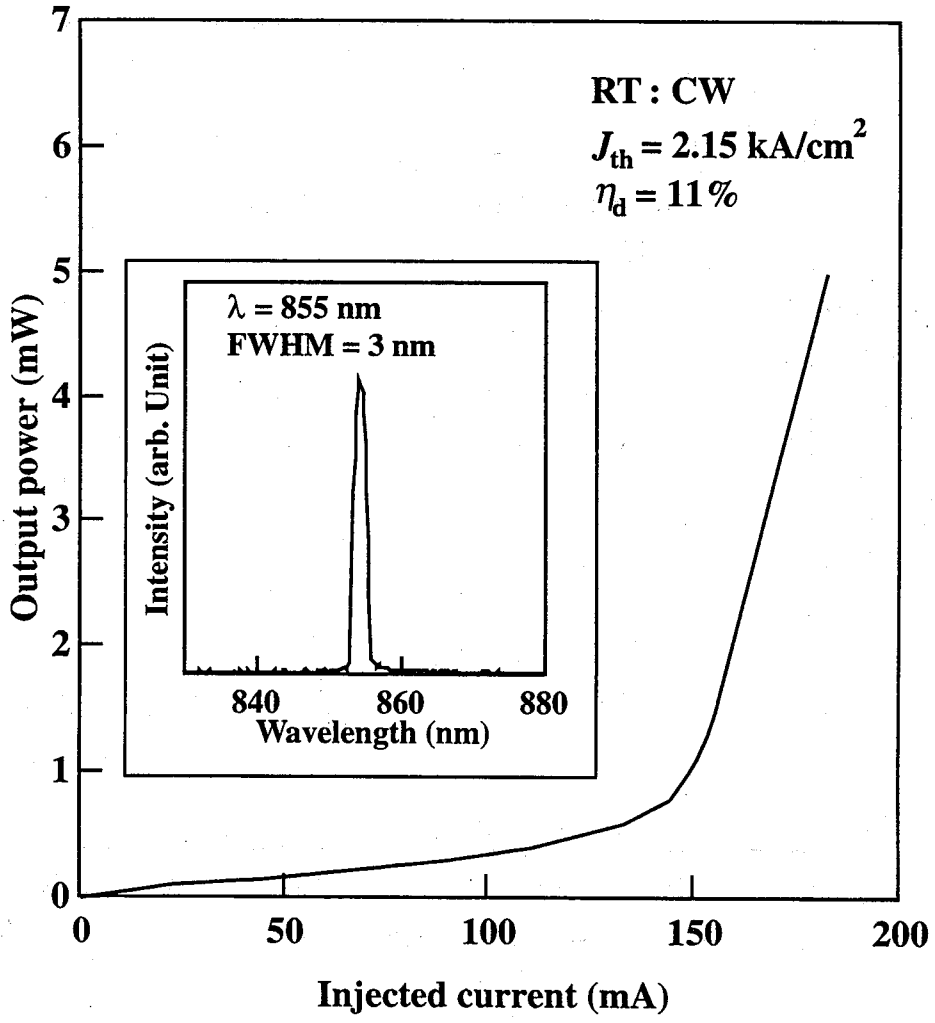

Figure 3.10 : *I-L* characteristics and emission spectrum of the $In_{0.1}Ga_{0.9}As$ QW laser on Si substrate.

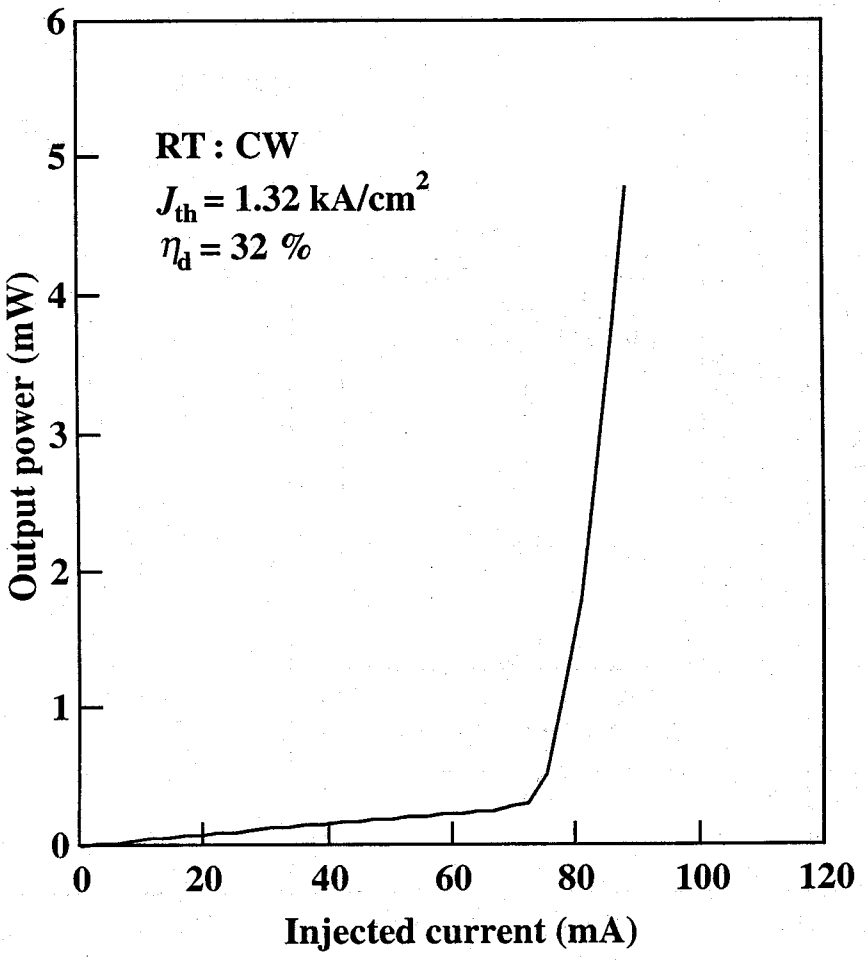

Figure 3.11 : Typical light output versus injected current characteristics of the $In_{0.2}Ga_{0.8}As$ quantum dot-like laser on a Si substrate at room temperature under the continuous wave condition.

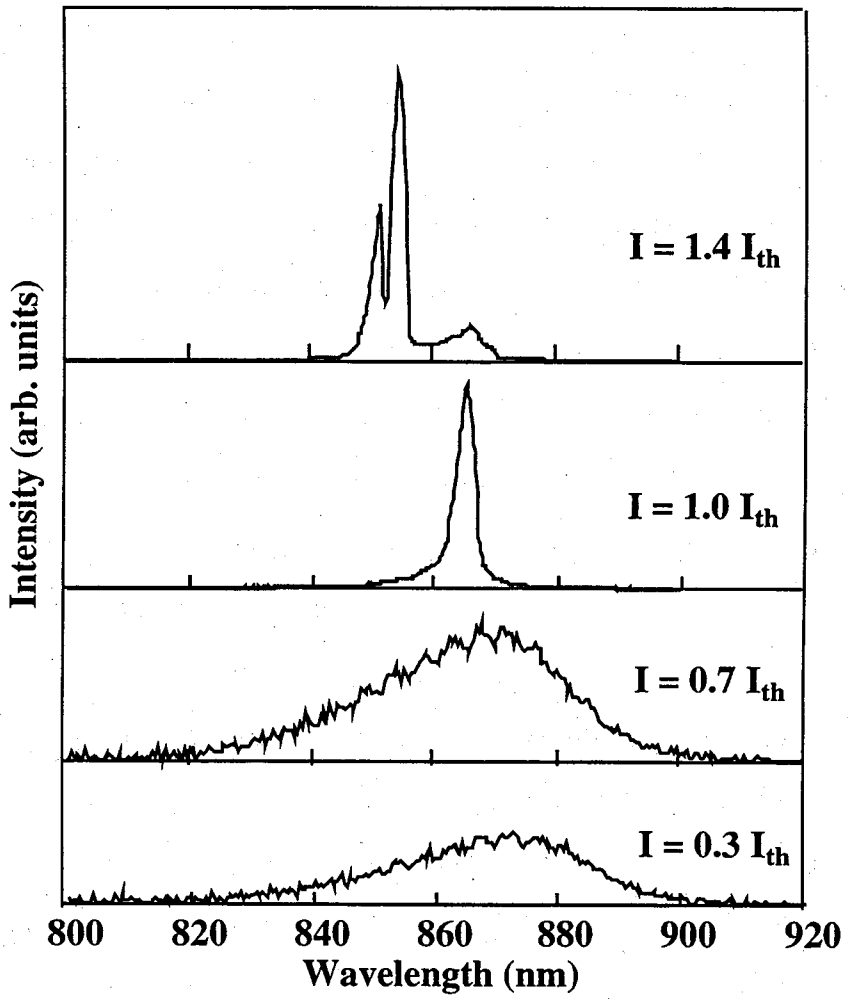

Figure 3.12 : Emission spectra of the $In_{0.2}Ga_{0.8}As$ quantum dot-like laser on a Si substrate at different curr ents.

the above said principle.

Figure 3.12 shows the applied current dependent emission spectra of $In_{0.2}Ga_{0.8}As$ QD-like laser on Si. Lasing starts at a threshold current of 1.4 I_{th} at a wavelength of 854 nm. Below the threshold current, the emission peak is observed at the wavelength of 872 nm. As the injection current increases, emission peak shifts from longer wavelength region to shorter wavelength region. However, the initially observed peak at longer wavelength region is appearing with extremely lower intensity. This is attributed to the reduction of the ground state gain of the dots as a result thermally activated carrier loss and the increased band-filling in the first excited state as the ground state gain becomes saturated[18].

I-L characteristics with emission spectrum for the $In_{0.3}Ga_{0.7}As$ and $In_{0.4}Ga_{0.6}As$ QD-like laser on Si under RT pulsed condition are shown in Fig. 3.13 and Fig. 3.14 respectively. The laser with $In_{0.3}Ga_{0.7}As$ QD-like active region shows a J_{th} of 1.51 kA/cm^2 with η_d 0f 7% (Fig. 3.13), while the laser with $In_{0.4}Ga_{0.6}As$ active region shows no lasing (Fig. 3.14) at RT pulsed mode. The failure of lasing in these lasers are due to the dot quality as with the increase of In content the size non-uniformity is severe. Further, the increase in In content in the active region increase the bending of threading dislocations caused by increasing strain[22-24]. The threading dislocations may also influence the carriers occupy higher energy levels and which can cause more severe non-radiative recombination and modulation of the losses by constructive interference with the reflection of a transverse leaky mode propagating in the transparent substrate. Thus decreases the radiative efficiency of the In rich QD-like dot lasers. The observed lasing emission with broad and splited peaks shown in Fig. 3.13 for $In_{0.3}Ga_{0.7}As$ QD-like active region is in agreement with the above discussion.

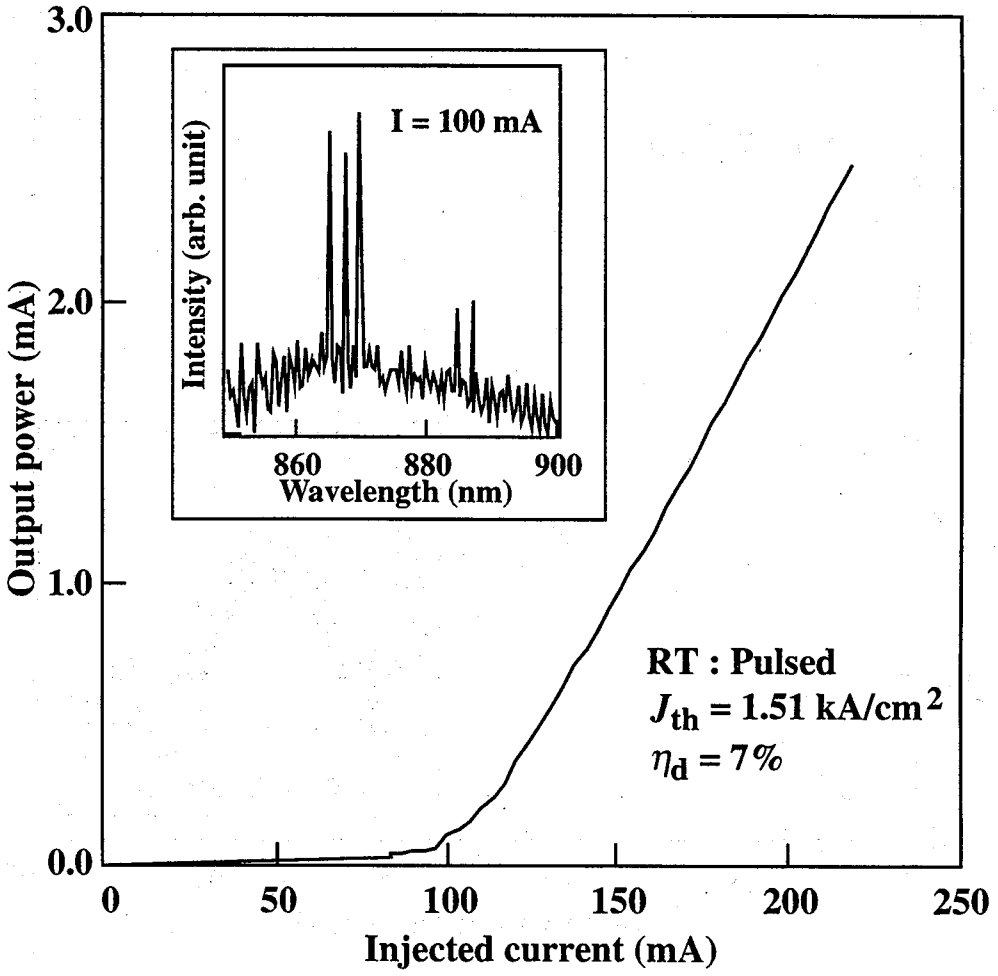

Figure 3.13 : I-L characteristics and emission spectrum of the $In_{0.3}Ga_{0.7}As$ QD-like laser on Si.

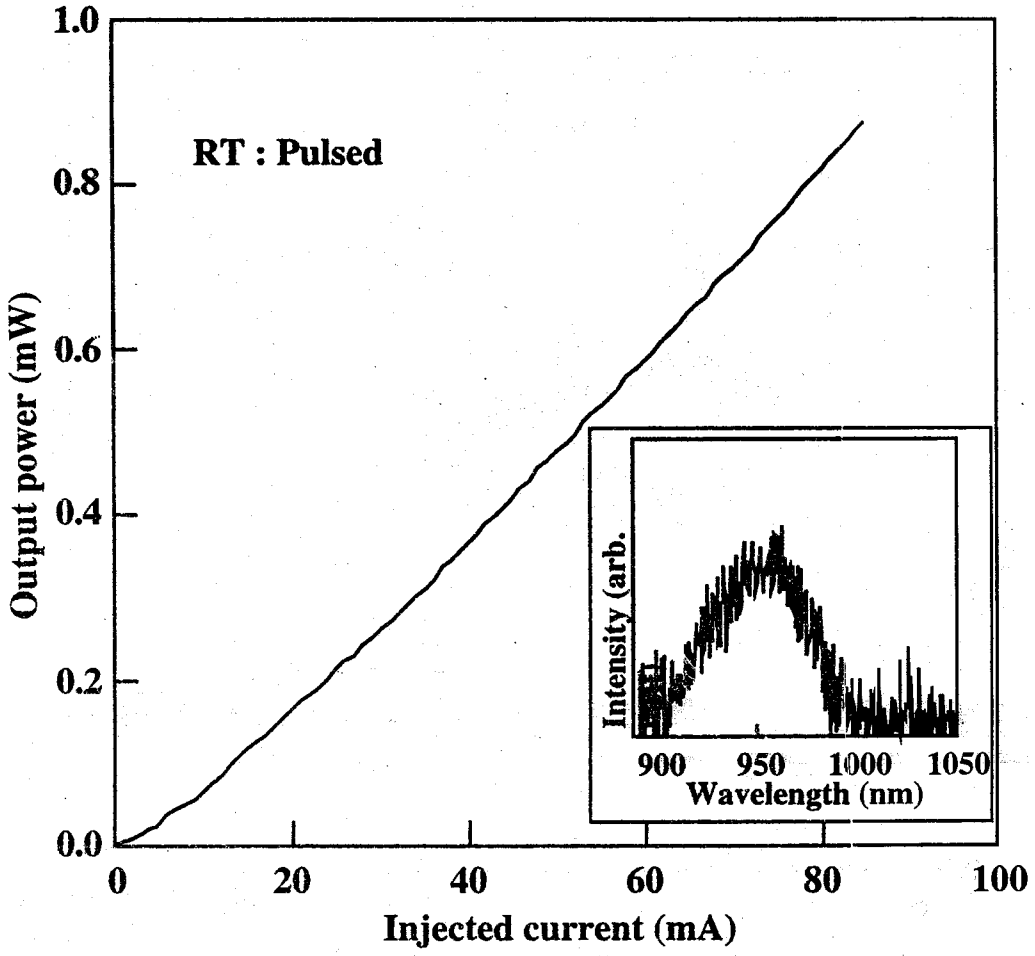

Figure 3.14 : I-L characteristics and emission spectrum of the $In_{0.4}Ga_{0.6}As$ QD-like laser on Si.

3.3.3 Aging behavior of QD-like laser diodes

The aging result under an APC condition for the $In_xGa_{1-x}As$ QD-like laser on Si is shown in Fig. 3.15. The lasers were operated at the CW constant output power of 0.5 mW and 2 mW at a heatsink temperature of 300 K. Though the laser with $In_{0.1}Ga_{0.9}As$ QD-like active region shows a poor reliability, the laser with $In_{0.2}Ga_{0.8}As$ QD-like active region shows an improved reliability. For this particular laser, first the operating current increased at a rate of ~ 1 mA/h for 78 h, after which a sudden increase was observed over the remaining lifetime of the device. Choi et al. demonstrated the longest lifetime of 56.5 h for a GaAs-based laser on Si with a strained $In_{0.05}Ga_{0.95}As$ active layer at a constant output power of 2 mW/facet at a heatsink temperature of 22°C[25]. In their case, the increase in operating current rate was 22 mA/h within the first hour and then decreased gradually up to 3 mA/h. After 10 h again increased gradually. Under the same condition, the present laser exhibits the longest lifetime of 27 h with an increase in threshold current rate of 1.9 mA/h for the first 20 h and 2.4 mA/h. After 27 h of operation, a sudden degradation is observed. The conventional GaAs-based laser on Si showed a rapid degradation only within a few minutes, due to the high order of dislocation density consisted by the active region. The <100> dark line defect (DLD) resulted from the formation of a complicated dislocation network due to the climbing motion from a dislocation that originally existed in the active region. Which believed from the origin of threading dislocation successively continued from the substrate during the crystal growth.

The gradual degradation at the earlier stage of aging test of the $In_{0.2}Ga_{0.8}As$ QD-like laser on Si indicates that the insertion of dot-like active region suppressed the formation of DLD or dark spot defects (DSDs). However, the failure of stability for longer duration is attributed to the elongation of the dislocation network towards the dot region from the non-dot region or gradual condensation of point defects in the dots or melting or destruction of the light

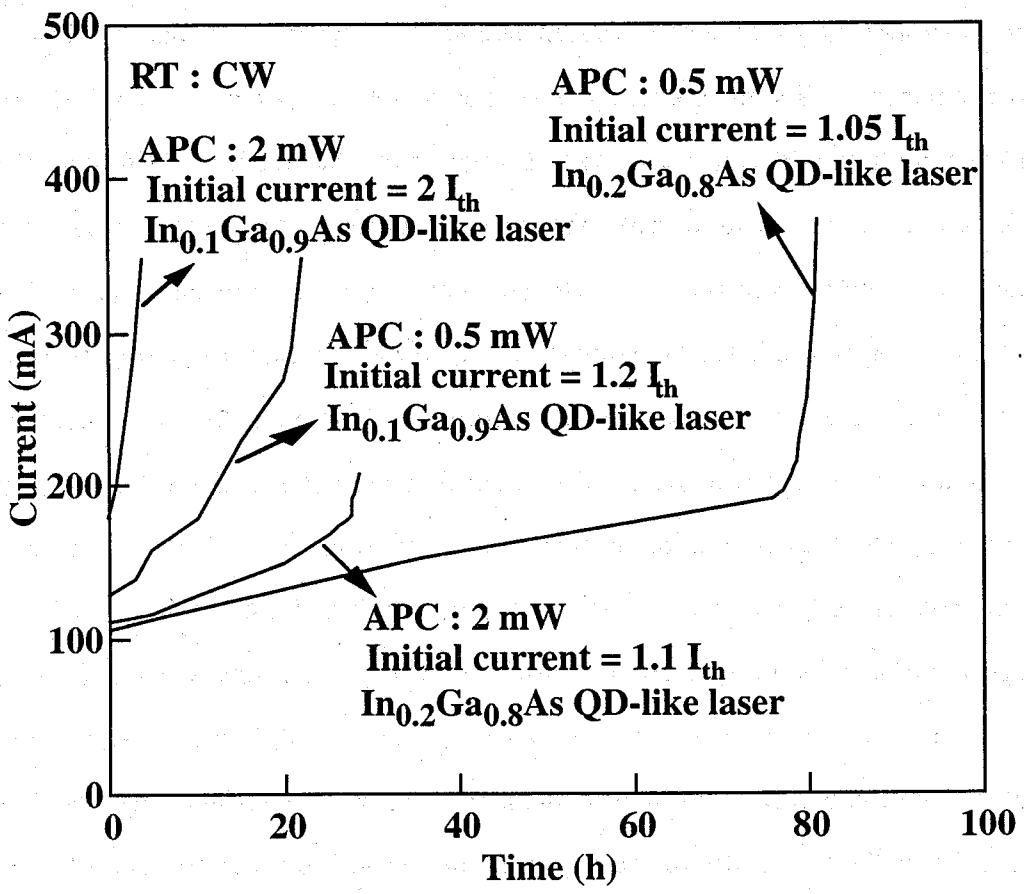

Figure 3.15 : Aging result of the $In_{0.2}Ga_{0.8}As$ quantum dot-like laser on a Si substrate at room temperature under the automatic power control condition.

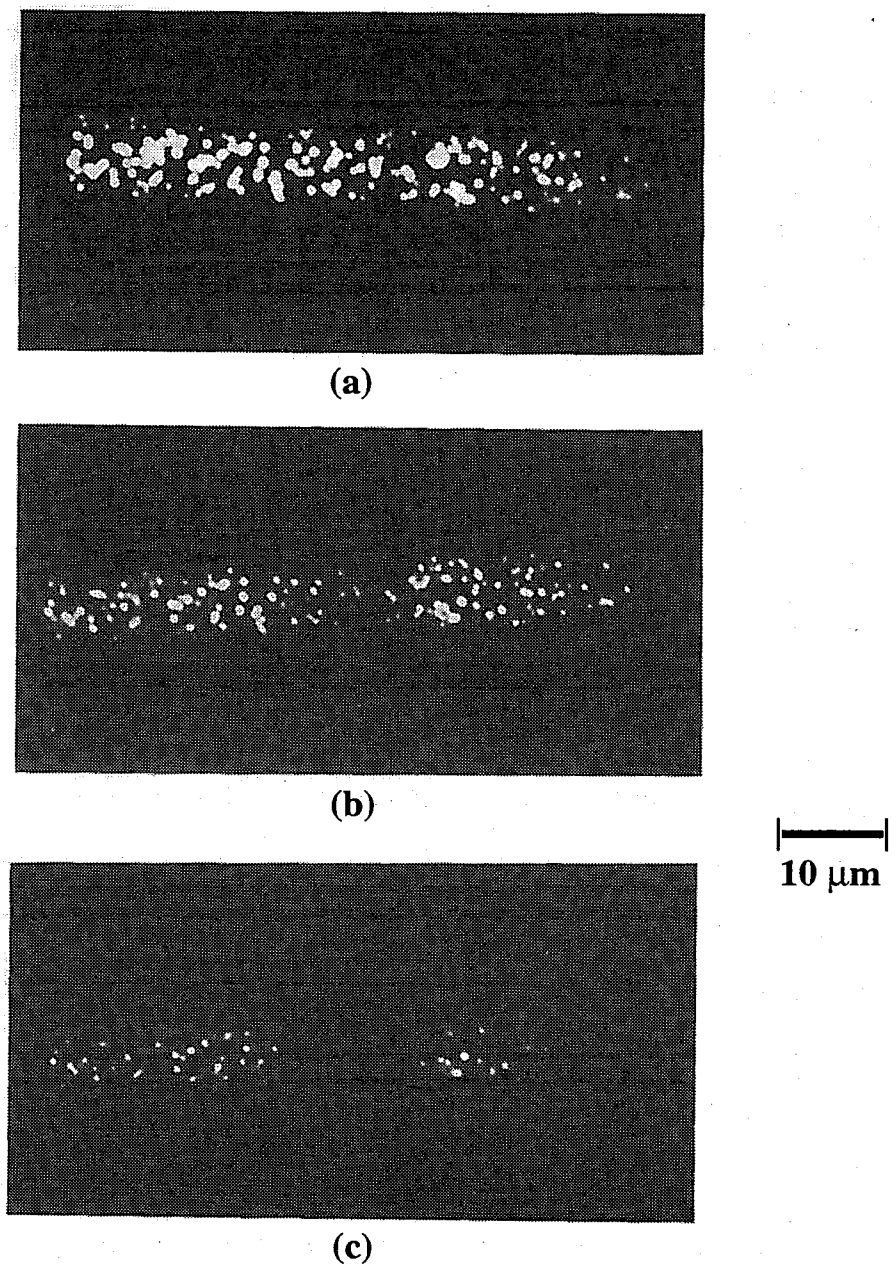

Figure 3.16 : Typical EL topographs of the $In_{0.2}Ga_{0.8}As$ QD-like laser on Si after (a) 1 hrs, (b) 6 hrs and (c) 12 hrs under dc operation at a constant current density of 1.3 kA/cm^2 at RT.

emitting part at the facet due to the joule heating.

Figure 3.16 (a-c) shows the typical EL topograph images of $In_{0.2}Ga_{0.8}As$ QD-like laser on Si under room temperature dc operation at a constant current density of 1.0 kA/cm^2 at different progressive stages of degradation. The electro-luminescence was found originating from the QD-like dot regions and gradual darkening appears in time of operation. The sources of dark spots are assumed as the dislocation sites existing around the dots. As the time of operation increases the dislocation sites starts to move along the current path and which finally reaches the active region and hinder the emission.

3.4. Conclusion

The growth conditions of QD-like dots on Si substrate by S-K growth mode have been optimized using MOCVD. QD-like structures were optimized by considering the growth temperature, V/III ratio and In content. Optimized QD-like structures were further used to fabricate laser diodes. $In_{0.2}Ga_{0.8}As$ QD-like active region showed room temperature CW light emission with a lowest threshold current density of 1.32 kA/cm^2 in our experiment. The shift of the lasing wavelength towards the shorter region of $In_{0.2}Ga_{0.8}As$ QD-like laser in comparison with the reported wavelength for InGaAs QW laser on GaAs was explained as an effect of In addition. The laser with $In_{0.3}Ga_{0.7}As$ QD-like active region showed a threshold current density of 1.51 kA/cm^2 under RT pulsed condition. Lasing emission was observed as broad and consists of splited peaks at a spaced interval due to the nonuniform distribution of the electronic states of the dots. The aging test of this laser revealed that this QD - like lasers are reliable than the QW lasers realized by the same structure on Si.

References

1. T. Egawa, A. Ogawa, T. Jimbo, and M. Umeno, Jpn. J. Appl. Phys., **37**, 1552 (1998).
2. Z. I. Kazi, T. Egawa, T. Jimbo, and M. Umeno, Jpn. J. Appl. Phys., **38**, 74 (1999).
3. I. N. Stransky and V. L. Krastanov, Akad. Wiss. Lit. Maniz. Natur. Kl. 11b, **146**, 797 (1939).
4. R. Notzel, N. N. Ledentsov, L. Daweritz, M. Hohenstein and K. Ploog, Phys. Rev. Lett., **67**, 3812 (1991).
5. R. Koch, M. Borbonus, O. Haase and K. H. Rieder, Phys. Rev. Lett., **67**, 3416 (1991).
6. V. A. Shchukin, A. I. Borovkov, N. N. Ledentsov and P. S. Kop'v, Phys. Rev., B **51**, 10104 (1995).
7. J. Tersoff and R. M. Tromp, Phys. Rev. Lett., 70, 2782 (1993).
8. V. Bressler-Hill, A. Lorke, S. Varma, P. M. Petroff, K. Pond and W. H. Weinberg, Phys. Rev. B **50**, 8479 (1994).
9. P. D. Wang, N. N. Ledentsov, C. M. Sotomayor Torres, P. S. Kop'ev and V. M. Ustinov, Appl. Phys. Lett., **64**, 1526 (1994).
10. R. Notzel, J. Temmyo and T. Tammamura, Nature (London), **369**, 131 (1994).
11. V. A. Shchukin, N. N. Ledentsov, P. S. Kop'ev and D. Bimberg, Phys. Rev. Lett., **74,** 4043 (1995).
12. V. A. Shchukin, N. N. Ledentsov, M. Grundmann, P. S. Kop'ev and D. Bimberg, V. M. Ustinov, Surf. Sci., **352-354**, 117 (1996).
13. M. Asada, Y. Miyamoto and Y. Suematsu, IEEE J. Quantum electron., **22**, 1915 (1986).
14. Y. Arakawa and H. Sakai, Appl. Phys. Lett., **40**, 939 (1982).
15. S. Farad, D. Leonard, J. L. Merz, and P. M. Petroff, Appl. Phys. Lett.,

65, 1388 (1994) .

16. J. Oshinowo, M. Nishioka, S. Ishida, and Y. Arakawa, Appl. Phys. Lett., **65**, 1421 (1994).
17. K. Mukai, N. Ohtsuka, H. Shoji and M. Sugawara, Appl. Phys. Lett., **68**, 3013 (1996).
18. D. G. Deppe, D. L. Huffaker, S. Csutak, Z. Zou, G. Park, and O. B. Shchekin, IEEE J. Quantum Electron., **35**, 1238 (1999).
19. G. Park, O. B. Shchekin and D. L. Huffaker, IEEE Photon. Tech. Lett., **13**, 230 (2000).
20. K. K. Linder, J. Phillips, O. Qasaimeh, X. F. Liu, S. Krisna, P. Bhattacharya and J. C. Jiang, Appl. Phys. Lett., **74**, 1355 (1999).
21. Y. Hasegawa, T. Egawa, T. Jimbo and M. Umeno, Jpn. J. Appl. Phys., **35**, 5637 (1996) .
22. J. J. Coleman and K. J. Beernink, J. Appl. Phys., **75**, 1879 (1994).
23. E. Yablonovitch and E. O. Kane, J. Lightwave Technol., 4, 504 (1986).
24. I. Suemune, IEEE J. Quantum Electron., 27, 1149 (1991).
25. H. K. Choi, C. A. Wang and N. H. Karam, Appl. Phys. Lett., **59**, 2634 (1991).